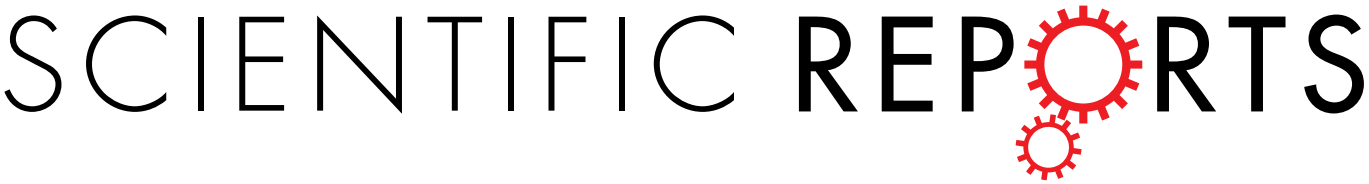

OPEN

Large reversible magnetocaloric effect in antiferromagnetic Ho_2O_3 powders

Received: 16 June 2017
Accepted: 9 October 2017
Published online: 24 October 2017

A. Boutahar[1], R. Moubah[2], E. K. Hlil[3], H. Lassri[2] & E. Lorenzo[3]

Giant magnetocaloric materials are highly promising for technological applications in magnetic refrigeration. Although giant magnetocaloric effects were discovered in first-order magnetic transition materials, it is accompanied by some non-desirable drawbacks, such as important hysteretic phenomena, irreversibility of the effect, or poor mechanical stability, which limits their use in applications. Here, we report the discovery of a giant magnetocaloric effect in commercialized Ho_2O_3 oxide at low temperature (around 2 K) without hysteresis losses. Ho_2O_3 is found to exhibit a second-order antiferromagnetic transition with a Néel temperature of 2 K. At an applied magnetic field change of 5T and below 3.5 K, the maximum value of magnetic entropy change ($-\Delta S_M^{max}$), the refrigerant capacity (RC) were found to be 31.9 $J.K^{-1}.kg^{-1}$ and 180 $J.K^{-1}$, respectively.

Cryocoolers able of cooling at low temperature (1.8–20 K) are widely utilized in different applications. As examples, they are used in hydrogen and helium liquefactions, superconducting quantum interference device (SQUID), medical instrumentation and diverse scientific research technologies. Superconducting magnet materials producing strong magnetic fields are broadly utilized in medicine and laboratories for scientific aims. Generally, liquid helium is used for cooling them, due to the fact that superconducting magnets exhibit low superconducting order temperature transition. However, liquid helium is expensive and scarcer which is not convenient from the economic point of view. Consequently, low-energy consumption cryocoolers are required. Magnetic refrigeration based on magnetocaloric effect (MCE) is a promising solution for refrigeration at low temperature[1–7]. Recently, considerable efforts were devoted to rare-earth based intermetallic compounds for low temperature magnetic refrigeration and some of them exhibit good MCE properties[8–16]. One of the main challenges in developing magnetic cryocoolers is to find a suitable working temperature range, large reversible magnetocaloric effect with low magnetic hysteresis losses. To date, the common used materials for cryogenic refrigeration[17–19] based on magnetocaloric effect[20–22] are hydrated salts. Such materials are used in low temperature cooling systems for detectors in space mission or laboratory facilities. The performance of an adiabatic demagnetization refrigerator (ADR)[23] is critically dependent on the design and construction of these salt pills that produce cooling. However, the only available salts refrigerants present some drawbacks because they are hydrated, which requires to be encapsulated in a hermetic container to prevent dehydration. Furthermore, hydrated salts are fabricated by growth which is not appropriate with industrial processes because it is very time consuming.

One can notice that for room temperature applications giant magnetocaloric effects (MCE) were reported in materials with a first-order magnetic transition (FOMT) such as $LaFe_{13-x}Si_x$[24–29] $Gd_5(Si,Ge)_4$[6] and others[30–32]. However, FOMTs occur in a narrow temperature window and are often accompanied with some non-desirable drawbacks such as the irreversibility of the MCE, very large thermal and magnetic-field hysteresis losses[33] and their high material cost. We note that very recently, the irreversibility of the MCE has been overcome in FOMT FeRh thin films[34] using dual-stimulus multicaloric cycle. It is known that magnetic materials with a second-order magnetic transition (SOMT) lack a very large ($-\Delta S_M$),[35–40] but they do present some advantages such as low magnetic hysteresis and tunable order temperature by varying composition. In this work, we found that commercialized Ho_2O_3 powders presents a giant magnetocaloric effect without magnetic hysteresis losses at low temperature.

[1]LabSIPE, Ecole Nationale des Sciences Appliquées, Université Chouaib Doukkali d'El Jadida, El Jadida, Plateau, 24002, Morocco. [2]LPMMAT, Université Hassan II-Casablanca, Faculté des Sciences Ain Chock, BP, 5366, Mâarif-Casablanca, Morocco. [3]Institut Néel, CNRS, Université Grenoble Alpes, 25 rue des Martyrs, BP, 166 38042, Grenoble cedex 9, France. Correspondence and requests for materials should be addressed to A.B. (email: boutahar.fsac@gmail.com)

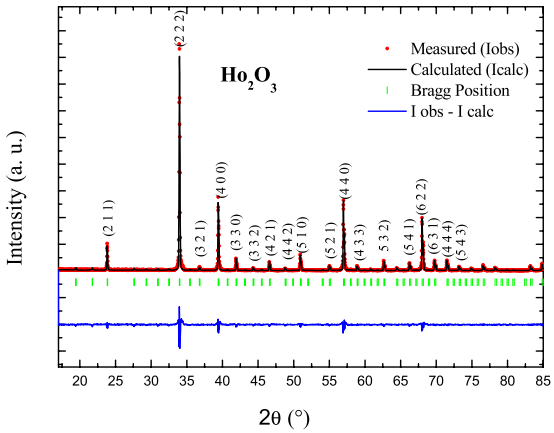

Figure 1. Rietveld refined powder XRD patterns of the Ho_2O_3 compound.

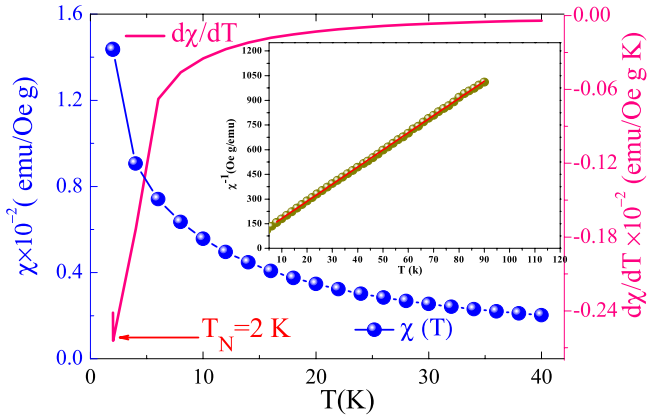

Figure 2. Change of the magnetic susceptibility and dχ/dT as a function of temperature recorded at an applied magnetic field of 0.05 T for Ho_2O_3 compound. Inset shows the inverse susceptibility versus temperature, symbol and solid line represent the experimental and linear fit obtained using Curie Weiss law.

Experimental Details

Holmium (II) oxide Ho_2O_3 polycrystalline powders (≥99.9% purity) was provided by Sigma Aldrich factory and heated at 1200 K for 48 hours. The crystalline structure was checked by x-ray diffraction (XRD) using D5000 Siemens diffractometer with Co-$K_{\alpha 1}$ radiation ($\lambda = 1.5406$ Å). Vibrating sample magnetometer (VSM)-quantum design was used to perform magnetic measurements at temperature ranging from 1.8 to 50 K, under an external applied magnetic field up to 5 T.

Results and Discussion

The XRD pattern of Ho_2O_3 powders is displayed in Fig. 1. Different diffraction peaks can be observed, indicating a polycrystalline character of the sample. All the diffraction peaks can be indexed according to the bixbyite structure, which is in agreement with the data found in the literature[41]. The lattice parameters were determined using Rietveld refinement and were found to be $a = b = c = 10.6186$ Å with $R_{WP} = 10.1\%$, $R_P = 12.18\%$ and $\chi^2 = 4.82$. The absence of any additional peak in the XRD pattern demonstrates that there are no spurious phases in the detection limit of XRD experiments. Figure 2 displays the temperature dependence of the magnetic susceptibility recorded at an applied magnetic field of 0.05 T for the Ho_2O_3 compound. As can be observed, the sample shows a decrease in magnetic susceptibility with increasing temperature which is associated with the antiferromagnetic interaction in Ho_2O_3 in agreement with previous reports[41]. In order to determine the Néel temperature (T_N), we display in the inset of Fig. 1(a) the $\chi = \frac{C}{T-\theta_P}$. versus T plot. The T_N is defined as the inflection point of derivative and it is around 2 K. Inset of Fig. 2 shows the change of magnetic susceptibility (χ^{-1}) as a function of temperature. In the paramagnetic region, χ^{-1}(T) was fitted using the classical Curie-Weiss law:

$$\chi = \frac{C}{T-\theta_P}. \tag{1}$$

where C is the Curie constant and θ_p is the Curie-Weiss temperature.

From the linear fit, the C and θ_p parameters were obtained. The negative ($\theta_p = -7$ K) value confirms the presence of an antiferromagnetic interaction. The C constant is related to the effective paramagnetic moment by the

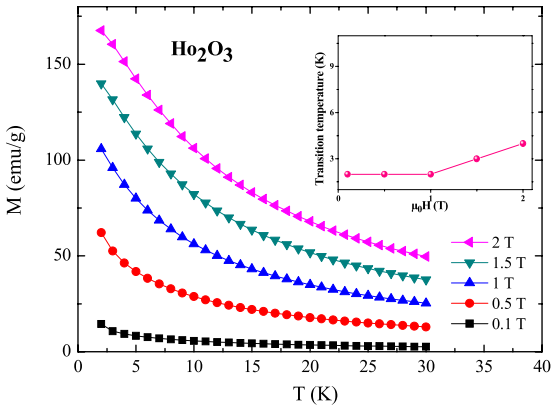

Figure 3. Temperature dependence of magnetization obtained at different magnetic fields ($\mu_0 H$) up to 2 T of the Ho_2O_3 compound. Inset shows the magnetic field dependence of transition temperature.

following relation $C = \frac{N_A \mu_{eff}^2}{3K_B}$; where $N_A = 6.023\ 10^{23}\ mol^{-1}$ is the Avogadro number, $\mu_B = 9.274\ 10^{-24}\ (A/m^2)$ is the Bohr magneton and k_B is the Boltzmann constant. From the determined C parameter, we have deduced the real effective moment of Ho value which was found to be $\mu_{eff}^{exp} = 11.8\,\mu_B$. The experimental effective paramagnetic moment μ_{eff}^{exp} is higher than the theoretical value ($\mu_{eff}^{the} = 10.6\,\mu_B$), which could be attributed to the crystal field effects which favors a high spin configuration[41].

Figure 3 shows the temperature dependence of the magnetization at different applied magnetic fields. We display in the inset of Fig. 3 the magnetic field dependence of transition temperature. As shown, the magnetic transition is sensitive to the high magnetic field. Sharp change of the M(T) curve can be observed with increasing temperature at low magnetic field, while the increase of the applied field leads to a broader distribution of the M (T) curve. With increasing applied magnetic field more magnetic moments are forced to follow the direction of the applied field, which induced a broader distribution of the M(T) curve.

Isothermal magnetization curves were measured at various temperatures (Fig. 4). The gradual evolution of these curves to linear behavior characterizes an increase of the paramagnetic contribution above T_N. Figure 4(b) presents the magnetic hysteresis loop of the Ho_2O_3 powder recorded at 2 K. The hysteresis loop is closed and completely reversible. These properties are highly suitable for magnetic refrigeration[42]. In order to investigate the nature of the magnetic phase transition, Arrott plots (H/M versus M^2) were studied (Fig. 5). According to the Banerjee criterion[43], a magnetic transition is the first-order when the slope of Arrott curves is negative, whereas it will be second-order when the slope is positive. As can be observed, positive slopes are observed for all temperatures which show that the H_2O_3 compound undergoes a SOMT.

The magnetocaloric effect can be related to the magnetic properties of the material through the thermodynamics Maxwell's relation. It has been calculated in terms of isothermal magnetic entropy change using isothermal magnetization obtained at various temperatures (Fig. 5). According to the thermodynamically theory[6], the isothermal magnetic entropy changes associated with a magnetic field change is given by:

$$\Delta S_M(T, \Delta H) = S_M(T, H) - S_M(T, 0) = \int_0^{\mu_0 H_{MAX}} \left(\frac{\partial S(T, H)}{\partial H}\right)_T H \tag{2}$$

From the Maxwell's thermodynamic relation

$$\left(\frac{\partial S(H, T)}{\partial H}\right)_T = \left(\frac{\partial M(H, T)}{\partial T}\right)_H \tag{3}$$

One can obtain the following expression

$$\Delta S_M(T, \Delta H)_{\Delta H} = \int_0^{\mu_0 H_{max}} \left(\frac{\partial M(H, T)}{\partial T}\right)_H dH. \tag{4}$$

Where $\mu_0 H_{max}$ is the maximum external field.

Figure 6 displays the temperature dependence of the magnetic entropy change of Ho_2O_3 powders obtained at different applied magnetic field changes (1, 2, 3, 4, and 5 T). For all fields, the $(-\Delta S_M)$ curves show a maximum at around 3 K, which it is close to T_N. We note that for a second-order phase transition the $(-\Delta S_M)(T)$ should show a peak with a maximum around T_N, however, since the T_N of the sample is too low (2 K), we only observe half peak of $(-\Delta S_M)(T)$. The peak magnitude increases when ΔH increases, from 8.2 to 31.9 J/kgK with increasing applied magnetic field change from 1 to 5 T, respectively. The large magnetocaloric effect in H_2O_3 can be understood by its high magnetization associated with its sharp magnetization change at the antiferromagnetic-paramagnetic and the presence of crystal field effects above the transition.

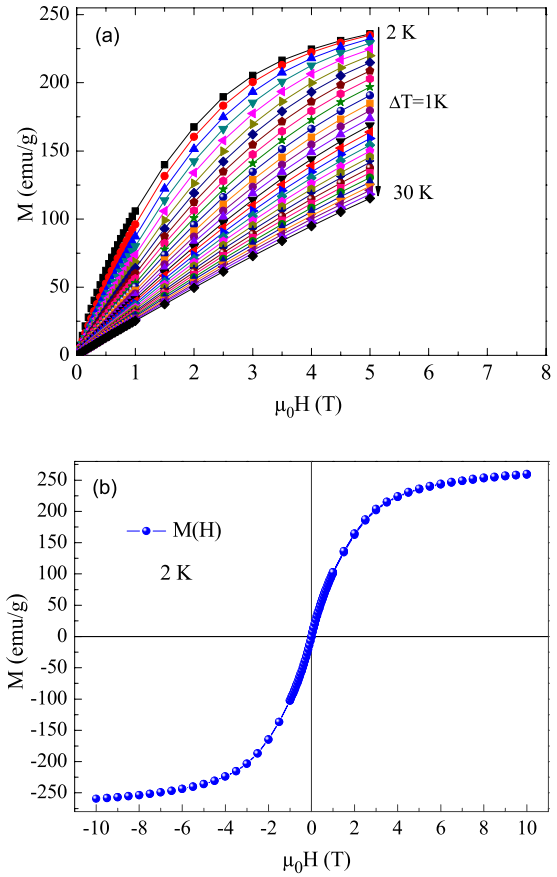

Figure 4. (**a**) Isothermal magnetization curves obtained at different temperatures from 2 to 30 K with an increment of 1 K of the Ho_2O_3 compound. (**b**) The full magnetization curve measured at transition temperature.

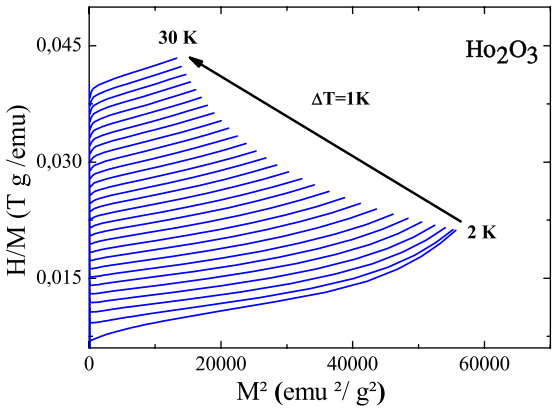

Figure 5. Arrott plots of the Ho_2O_3 compound.

Other important parameters of refrigerant materials are the refrigerant capacity RC and the adiabatic temperature change ΔT_{ad}. According to Wood and Potter[44] the RC of a reversible refrigeration cycle operating between T_h and T_c (temperatures of the hot and cold reservoirs, respectively) is defined as $RC = (-\Delta S_M) \times \Delta T$, where $(-\Delta S_M)$, is the magnetic entropy change at the hot and cold ends of the cycle and $\Delta T = T_h - T_c$. For magnetic field changes of 0–4 T and 0–5 T, the values of RC were estimated to be 165 and 180 J/kg, respectively.

ΔT_{ad} can be calculated from magnetization and heat capacity measurements C_p[6]

$$\Delta T_{ad} = \mu_0 \int_0^{\mu_0 H} \frac{T}{C_p} \left(\frac{\partial M}{\partial T}\right)_H dH \quad (5)$$

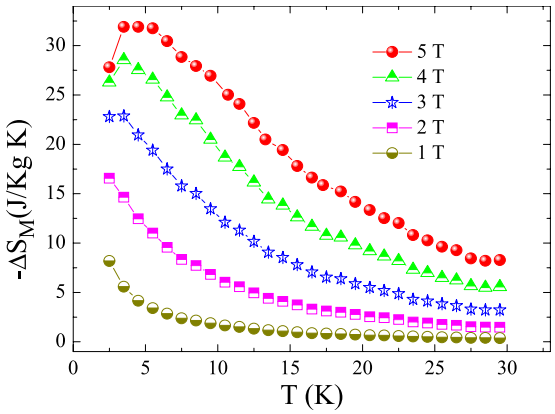

Figure 6. Temperature dependence of magnetic entropy change ($-\Delta S_M$) under different magnetic field changes 1, 2, 3, 4, and 5 T of the Ho_2O_3 compound.

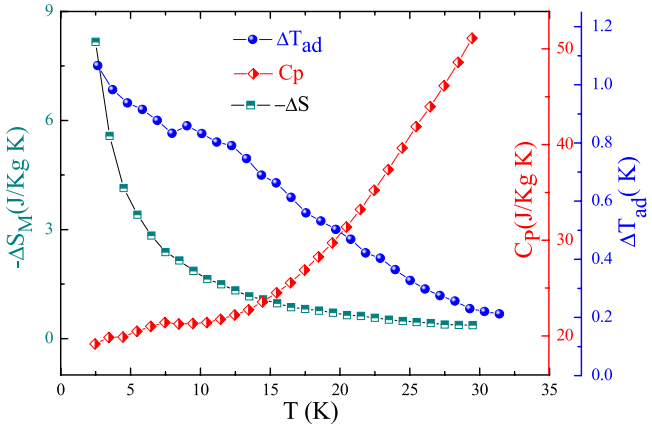

Figure 7. Temperature dependence of magnetic entropy change ($-\Delta S_M$), heat capacity and adiabatic temperature change ΔT_{ad} under magnetic field changes 1 T of the Ho_2O_3 compound.

Material	$T_{C,N}$ (K)	$-\Delta S_m^{max}$ (J/kg K)	RC (J/kg)	Ref.
Ho_2O_3	2	31.9	180	This work
Ho_3Al_2	40	18.7	—	47
$Ho_{30}Y_{26}Al_{24}Co_{20}$	5.5	10.76	241	48
TmZn	8.4	26.9	214	49
ErRuSi				
	8	21.2	—	50
$ErMn_2Si_2$	4.5	25.2	—	51
$HoCu_2O_5$	14	9.2	—	13
$HoNiAl_2$	7.5	14	171	14
TmZnAl	2.8	9.4	149	15

Table 1. Magnetic ordering temperature ($T_{N,C}$), maximum values of ($-\Delta S_M^{max}$) and refrigerant capacity (RC) under the magnetic field change of 5 T of the Ho_2O_3 compound and some potential magnetic refrigerant materials.

The temperature dependence of ΔT_{ad} and heat capacity for magnetic field changes of 1 T is shown in Fig. 7. It can be seen that ΔT_{ad} increases with decreasing temperature. The maximum values of adiabatic temperature change (ΔT_{ad}^{max}) reaches 1.08 K for a magnetic field change of 1 T.

In order to examine the usefulness of the Ho_2O_3 compound reported in this work, we made a comparative study of $T_{N,C}$, ($-\Delta S_M^{max}$), RC with other magnetocaloric materials found in literature with low temperature magnetic transitions. The comparison is summarized in Table 1. It can be concluded that ($-\Delta S_M^{max}$) is larger or comparable to those of reported potential magnetic refrigerant materials,[13–15,45–51]. However, the ordering temperature of Ho_2O_3

compound is smaller than the other materials. We note that the RC factor is comparable or smaller than those of the materials reported in Table 1. The giant values of $(-\Delta S_M)$, the low-cost and fast way of preparation suggest that this compound is one suitable candidate as a magnetic refrigerant in low temperature range (around 2 K).

Conclusion

In this paper, we have studied the magnetic and magnetocaloric properties of Ho_2O_3 powders. Magnetic measurements have shown the presence of an antiferromagnetic–paramagnetic transition around 2 K and a giant magnetic entropy change with second-order magnetic transition. Strong influence of crystal field effect is also observed in magnetic properties as well as magnetocaloric effect. Our study demonstrates that the Ho_2O_3 material could be considered as a potential candidate for magnetic refrigeration applications at low temperature (around 2 K).

References

1. Debye, P. Einige Bemerkungen zur Magnetisierung bei tiefer Temperatur. *Ann. Phys.* **386**, 1154–1160 (1926).
2. Giauque, W. F. A thermodynamic treatment of certain magnetic effects. A proposed method of producing temperatures considerably below 1° absolute. *J. Am. Chem. Soc.* **49**, 1864–1870 (1927).
3. Giauque, W. F. & MacDougall, D. P. Attainment of temperatures below 1° absolute by demagnetization of $Gd_2(SO_4)_3\,8H_2O$. *Phys. Rev.* **43**, 768 (1933).
4. Li, L. W. Review of magnetic properties and magnetocaloric effect in the intermetallic compounds of rare earth with low boiling point metals. *Chin. Phys. B* **25**, 037502 (2016).
5. Li, L. W., Hu, G., Qi, Y. & Umehara, I. Hydrostatic pressure effect on magnetic phase transition and magnetocaloric effect of metamagnetic TmZn compound. *Sci. Rep.* **7**, 42908 (2017).
6. Zhang, Y. *et al.* Excellent magnetocaloric properties in RE_2Cu_2Cd (RE = Dy and Tm) compounds and its composite materials. *Sci. Rep.* **6**, 34192 (2016).
7. Li, L. W. *et al.* low field magnetocaloric effect and field-induced metamagnetic transition in TmZn. *Appl. Phys. Lett.* **104**, 092416 (2014).
8. Yang, Y. *et al.* Magnetic and magnetocaloric properties of the ternary cadmium based intermetallic compounds of Gd_2Cu_2Cd and Er_2Cu_2Cd. *J. Alloys Compd* **692**, 665–669 (2017).
9. Yalin, Y., Li, L. W., Kunpeng, S., Yang, Q. & Dexuan, H. Large magnetocaloric effect in a wide temperature range induced by two successive magnetic phase transitions in Ho_2Cu_2Cd compound. *Intermetallics* **80**, 22 (2017).
10. Zhang, Y. *et al.* Large reversible magnetocaloric effect in RE_2Cu_2In (RE = Er and Tm) and enhanced refrigerant capacity in its composite materials. *J. Phys. D: Appl. Phys* **49**, 145002 (2016).
11. Zhang, Y. *et al.* Study of the magnetic phase transitions and magnetocaloric effect in Dy_2Cu_2 In compound. *J. Alloys Compd.* **667**, 130–133 (2016).
12. Li, L. W., Namiki, T., Huo, D., Qian, Z. & Nishimura, K. Two successive magnetic transitions induced large refrigerant capacity in HoPd In compound. *Appl. Phys. Lett.* **103**, 222405 (2013).
13. Li, L. W. *et al.* Magnetic properties and magnetocaloric effect in metamagnetic $RE_2Cu_2O_5$ (RE = Dy and Ho) cuprates. *J. Alloy Comp* **658**, 500 (2016).
14. Zhang, Y. *et al.* Magnetic properties and magnetocaloric effect in the aluminide $RENiAl_2$ (RE = Ho and Er) compounds. *Intermetallics* **88**, 61 (2017).
15. Zhang, Y. *et al.* Magnetic properties and magnetocaloric effect in TmZnAl and TmAgAl compounds. *J. Alloys. Comp.* **656**, 635 (2016).
16. Boutahar, A. *et al.* Magnetocaloric effect in $CoEr_2$ intermetallic compound. *J. Magn. Magn. Mater.* **444**, 106 (2017).
17. Evangelisti, M. *et al.* Cryogenic Magnetocaloric Effect in a Ferromagnetic Molecular Dimer. Ang. *Chem. Int. Ed.* **50**, 29 (2011).
18. Li, J. *et al.* Enhanced Cryogenic Magnetocaloric Effect Induced by Small Size $GdNi_5$ Nanoparticles. *J. Mater. Sci. Technol.* **30**, 973 (2014).
19. Barclay, A. & Steyert, W. A. Materials for magnetic refrigeration between 2 K and 20 K. *Cryogenics* **22**, 73 (1982).
20. Gschneidner, K. A., Pecharsky, V. K. & Tsoko, A. O. Recent developments in magnetocaloric materials. *Rep. Prog. Phys.* **68**, 1479 (2005).
21. Pecharsky, V. K. & Gschneidner, K. Magnetocaloric effect from indirect measurements: Magnetization and heat capacity. *J. Appl. Phys.* **86**, 565 (1999).
22. Pecharsky, V. K. & Gschneidner, K. A. Giant Magnetocaloric Effect in $Gd_5(Si_2Ge_2)$. *Phys. Rev. Lett.* **78**, 4494 (1997).
23. Jang, D. *et al.* Large magnetocaloric effect and adiabatic demagnetization refrigeration with $YbPt_2Sn$. *Nat. Commu.* **6**, 8680 (2015).
24. Boutahar, A., Phejar, M., Boncour, M. V., Bessais, L. & Lassri, H. Theoretical Work in Magnetocaloric Effect of $LaFe_{13-x}Si_x$ Compounds. *J. Supr. Cond. Novel Magn.* **27**, 5 (2014).
25. Rosca, M. *et al.* Neutron diffraction study of $LaFe_{11.31}Si_{1.69}$ and $LaFe_{11.31}Si_{1.69}H_{1.45}$ compounds. *J. Alloys Comp.* **490**, 50 (2010).
26. Fujita, A., Fujieda, S., Fukamichi, S. K., Mutamira, H. & Goto, T. Itinerant-electron metamagnetic transition and large magnetovolume effects in $La(Fe_xSi_{1-x})_{13}$ compounds. *Phys. Rev. B.* **65**, 014410 (2001).
27. Hu, F.-X., Shen, B.-G., Sun, J.-R. & Cheng, Z.-H. Influence of negative lattice expansion and metamagnetic transition on magnetic entropy change in the compound $LaFe_{11.4}Si_{1.6}$. *Appl. Phys. Lett.* **78**, 3675 (2001).
28. Balli, M., Rosca, M., Fruchart, D. & Ginoux, D. Effect of interstitial nitrogen on magnetism and entropy change of $LaFe_{11.7}Si_{1.3}$ compound. *J. Magn. Magn. Mater.* **321**, 123 (2009).
29. Boutahar, A., Zehani, K., Bessais, L., Lassri, H. & Hlil, E. K. Influence of bismuth on magnetism and magnetocaloric properties of $LaFe_{11.6}Si_{1.4}$ intermetallic compound. *J. Rare Earth* **33**, 740 (2015).
30. Gschneidner, K. A. & Pecharsky, V. K. Magnetocaloric Materials. *Annu. Rev. Mater. Sci.* **30**, 387 (2000).
31. Tegus., O., Brück., E., Buschow, K. H. & Boer., F. R. Transition-metal-based magnetic refrigerants for room-temperature applications. *Nature (London)* **415**, 150 (2002).
32. Franco., V., Blazquez, J. S., Ingale, B. & Conde, A. The Magnetocaloric Effect and Magnetic Refrigeration Near Room Temperature: Materials and Models. *Annu. Rev. Mater. Res.* **42**, 305 (2012).
33. Provenzano, V., Shapiro, A. J. & Shull, R. D. Reduction of hysteresis losses in the magnetic refrigerant Gd5Ge2Si_2 by the addition of iron. *Nature (London)* **429**, 853 (2004).
34. Liu, Y., et al. Large reversible caloric effect in FeRh thin films via a dual-stimulus multicaloric cycle. *Nature Commun*, https://doi.org/10.1038/ncomms11614 (2016).
35. Boutahar., A. *et al.* The Influence of Vanadium on Magnetism and Magnetocaloric Properties of $Fe_{80-x}V_xB_{12}Si_8$ (x = 8, 10, and 13.7) Amorphous Alloys, J. Suprcond. *Novel Magn.* **27**, 2401 (2014).
36. Chen., J., Shen, B. G., Dong, Q. Y., Hu, F. X. & Sun, J. R. Giant reversible magnetocaloric effect in metamagnetic HoCuSi compound. *Appl. Phys. Lett.* **96**, 152501 (2010).
37. Bonilla, C. M. *et al.* Universal behavior for magnetic entropy change in magnetocaloric materials: An analysis on the nature of phase transitions. *Phys. Rev. B* **81**, 224424 (2010).

38. Boutahar, A., Lassri, H. & Hlil, E. K. Low Temperature Giant Magnetocaloric Effect and Critical Behavior in Amorphous $Co_{100-x}Er_x$ (x = 55, 65) Alloys. J. Supr. Cond. *Novel Magn.* **27**, 2865 (2014).
39. Plaza., E. J. R., Sousa., V. S. R., Reis., M. S. & Von Ranke., P. J., A comparative study of the magnetocaloric effect in RNi_2 (R = Dy, Ho, Er) intermetallic compounds. *J. Alloys Comp* **505**, 357 (2010).
40. Moubah, R. *et al*. Enhanced magnetocaloric properties of FeZr amorphous films by C ion implantation. *Mater. Lett.* **175**, 5 (2016).
41. Heiba, Z. K., Bakr & Mohamed, M. Structural and magnetic properties of Mn doped Ho_2O_3 nanocrystalline. *J. Mol. Str.* **1102**, 140 (2015).
42. Boutahar., A., Lassri., H. & Hlil., E. K. Magnetic, magnetocaloric properties and phenomenological model in amorphous $Fe_{60}Ru_{20}B_{20}$ alloy. Solid Stat. *Commun.* **221**, 9 (2015).
43. Banerjee, B. K. On a generalised approach to first and second order magnetic transitions. *Phys. Lett.* **12**, 16 (1964).
44. Wood, M. E. & Potter, W. H, General analysis of magnetic refrigeration and its optimization using a new concept: maximization of refrigerant capacity. *Cryogenics* **25**, 667 (1985).
45. Li, L. W. & Nishimura, K. Giant reversible magnetocaloric effect in antiferromagnetic superconductor $Dy_{0.9}Tm_{0.1}Ni_2B_2CDy_{0.9}Tm_{0.1}Ni_2B_2C$ compound. *Appl. Phys. Lett.* **95**, 132505 (2009).
46. Hermes, W., Rodewals, U. C. & Pottgen, R. Large reversible magnetocaloric effect due to a rather unstable antiferromagnetic ground state. *J. Appl. Phys.* **108**, 113919 (2010).
47. Zhang, H. *et al*. Giant magnetic refrigerant capacity in Ho_3Al_2 compound. *Solid State Comm.* **152**, 1127 (2012).
48. Luo, Q., Zhao, D. Q., Pan, M. X. & Wang, W. H. Magnetocaloric effect of Ho-, Dy and Er-based bulk metallic glasses in helium and hydrogen liquefaction temperature range, App. *Phy. Lett.* **90**, 211903 (2007).
49. Li, L. W. *et al*. Giant low field magnetocaloric effect and field-induced metamagnetic transition in TmZn. *Appl. Phys. Lett.* **107**, 132401 (2015).
50. Gupta, S. B. & Suresh, K. G. Giant low field magnetocaloric effect in soft ferromagnetic ErRuSi. *Appl. Phys. Lett.* **102**, 022408 (2013).
51. Li, L. *et al*. Giant reversible magnetocaloric effect in $ErMn_2Si_2$ compound with a second order magnetic phase transition. *Appl. Phys. Lett.* **100**, 152403 (2012).

Acknowledgements

This work is mainly supported by the PHC Maghreb 15MAG07.

Author Contributions

A.B. and E.K.H. performed experiments and wrote the manuscript. R.M., H.L. and E.L. guided for writing the manuscript and provided financial aids through their projects.

Additional Information

Competing Interests: The authors declare that they have no competing interests.

Publisher's note: Springer Nature remains neutral with regard to jurisdictional claims in published maps and institutional affiliations.